ACS APPLIED MATERIALS & INTERFACES

Research Article

www.acsami.org

Flexible and Disposable Sensing Platforms Based on Newspaper

MinHo Yang,[‡,†] Soon Woo Jeong,[‡,†] Sung Jin Chang,[§] Kyung Hoon Kim,[‡] Minjeong Jang,[‡] Chi Hyun Kim,[‡] Nam Ho Bae,[‡] Gap Seop Sim,[∥] Taejoon Kang,[⊥,#] Seok Jae Lee,[*,‡] Bong Gill Choi,[*,▽] and Kyoung G. Lee[*,‡]

[‡]Nanobio Application Team, National NanoFab Center (NNFC), Daejeon 34141, Republic of Korea

[§]Department of Chemistry, Chung-Ang University, Seoul 06911, Republic of Korea

[∥]Fusion Process Technology Team, National NanoFab Center (NNFC), Daejeon 34141, Republic of Korea

[⊥]Hazards Monitoring Bionano Research Center and BioNano Health Guard Research Center, Korea Research Institute of Bioscience & Biotechnology, Daejeon 34141, Republic of Korea

[#]Major of Nanobiotechnology and Bioinformatics, University of Science and Technology, Daejeon 34113, Republic of Korea

[▽]Department of Chemical Engineering, Kangwon National University, Samcheok 25913, Republic of Korea

Supporting Information

ABSTRACT: The flexible sensing platform is a key component for the development of smart portable devices targeting healthcare, environmental monitoring, point-of-care diagnostics, and personal electronics. Herein, we demonstrate a simple, scalable, and cost-effective strategy for fabrication of a sensing electrode based on a waste newspaper with conformal coating of parylene C (P-paper). Thin polymeric layers over cellulose fibers allow the P-paper to possess improved mechanical and chemical stability, which results in high-performance flexible sensing platforms for the detection of pathogenic *E. coli* O157:H7 based on DNA hybridization. Moreover, P-paper electrodes have the potential to serve as disposable, flexible sensing platforms for point-of-care testing biosensors.

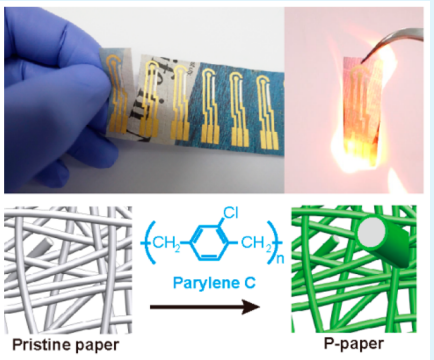

KEYWORDS: *Paper, foodborne pathogen, electrochemical electrode, parylene C, biosensor*

INTRODUCTION

Flexible technology is leading to a new era in the IT industry, as it allows the manufacture of flexible displays,[1] artificial skins,[2] and flexible electronics.[3] Numerous concepts for flexible sensors have been proposed and are being recognized as key components of smart portable devices targeting healthcare,[4,5] environmental monitoring,[6] point-of-care diagnostics,[7] and personal electronics.[4,5,7] To realize flexible sensors, many fabrication processes have been devised, such as the coating of active materials on flexible substrates involving plastics,[8] papers,[9−12] and textiles[6] that replace conventional rigid and planar counterparts. Thus, fully flexible platforms with excellent mechanical strength, controlled wettability and functionality, and unique morphologies (e.g., porosity) are required for sensing applications. Recent research has focused mainly on means of producing nanostructured electrochemical active materials, and rather less attention has been paid to technology platforms, even though their features can substantially affect sensor performance.

Of the various platforms used to date, paper is probably the cheapest and most widely used flexible and eco-friendly substrate in daily life, and it includes writing, wiping, wrapping, and packaging applications.[13−15] Paper is a sheet material produced by pressing moist lignocellulosic microfibers together, and papers exhibit chemical stability, strong mechanical strength, biodegradability, functionality, and permeability.[13] These attractive features make paper a promising platform for the construction of flexible devices, such as electronics,[16] microfluidic devices,[17] energy storage,[18] gas sensors,[19] biosensors,[20,21] and piezoelectric papers.[22] In particular, the porous nature of paper, which originates from interconnected wood cellulose fibers, is useful for electrochemical applications (e.g., energy storage and electrochemical sensors), and in combination with high specific surface area allows efficient and rapid mass transport, and enhanced electrochemical performance.[6,13,21,23] However, when paper is wet, its mechanical properties are badly affected.[24] Furthermore, although paper porosity is attractive in terms of electrochemical reactions, the high porosities and surface roughness of common papers limit good electrical connections with metal nanoparticle lines deposited on paper.[25] In order to use paper as a platform, some surface treatment is required, and various materials, such

Received: August 16, 2016
Accepted: December 5, 2016
Published: December 5, 2016

DOI: 10.1021/acsami.6b10298
ACS Appl. Mater. Interfaces 2016, 8, 34978−34984

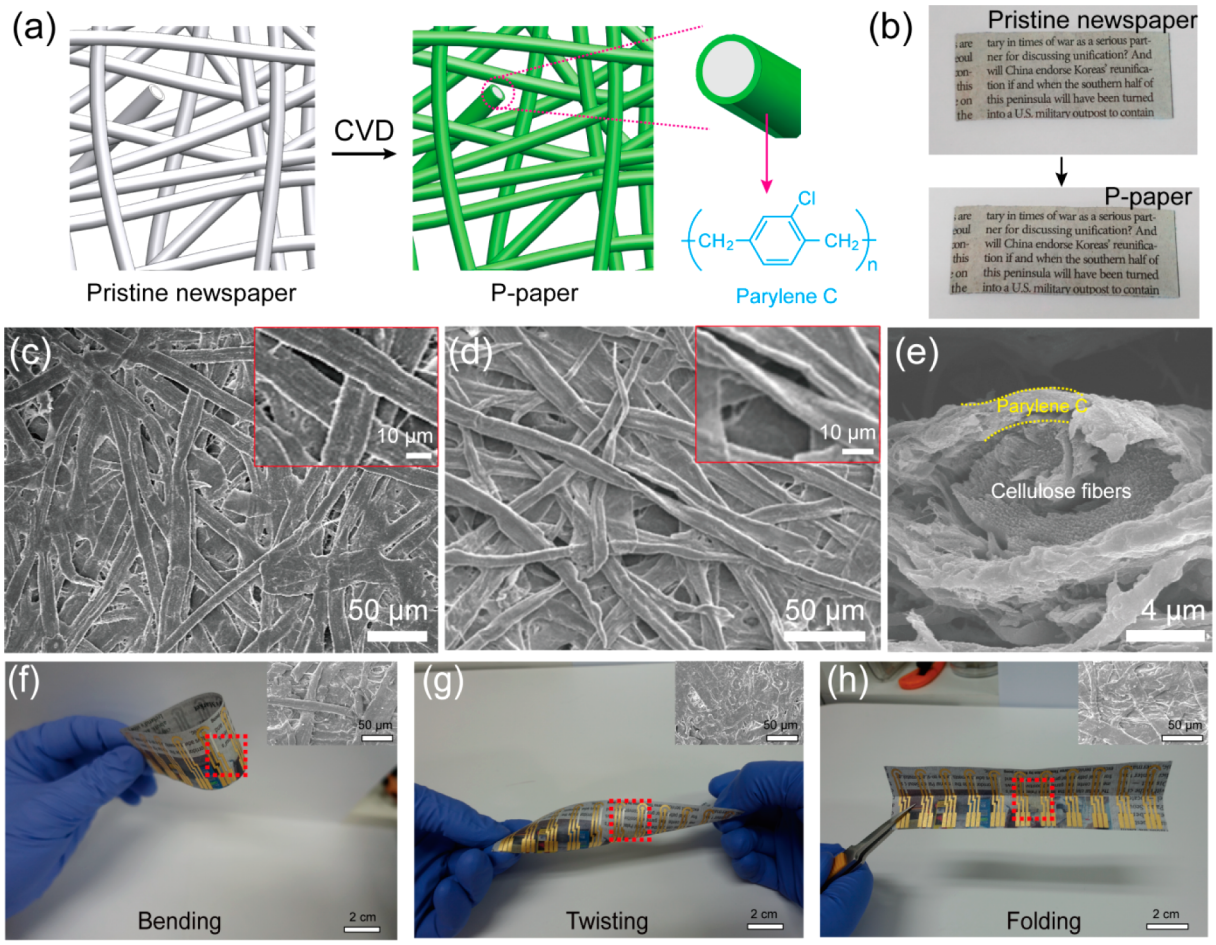

Figure 1. (a) Schematic illustration of fabrication process of P-paper. (b) Photographs of pristine newspaper and P-paper. Top-view SEM images of (c) pristine newspaper and (d) P-paper. (e) Cross-sectional SEM image of P-paper. Photographs of P-paper after (f) bending, (g) twisting, and (h) folding. (Insets show SEM images for each from the samples.)

as wax, organic/inorganic polymers, and ceramics, have been extensively investigated to determine how they modify paper surfaces (e.g., wettability, functionality, and roughness).[26−31] In most cases, solution-based coating methods have been adopted, but these methods often require a complicated experimental procedure, involving polymer synthesis, a coating process, and curing step.[32] Moreover, surface tension effects when solution-based methods are used lead to poor coating conformity and may bury the porous structure of papers.[33]

Herein, we developed a simple and scalable process for the fabrication of flexible and disposable sensor platforms based on coating the surface of paper with parylene C by chemical vapor deposition (CVD). A parylene C coating was selected as barrier layer for fabrication of paper electrodes because of its low surface energy (19.6 mN m^{-1}) and low stick coefficient (<1 × 10^{-3} at room temperature).[34] In addition, because CVD is a dry and single step process, it enables an efficient approach for a conformal surface modification and enhances mechanical properties as well as increases the hydrophobicity of paper while maintaining its porous nature.[35−37] Using waste newspaper as a flexible and disposable sensor platform, we were able to fabricate a sensing electrode via patterning of gold and silver layers on parylene-C-coated paper (P-paper). Produced paper electrodes were applied in an electrochemical pathogen sensor and showed excellent electrochemical performances with considerable potential as biosensor platforms for point-of-care testing biosensors.

EXPERIMENTAL SECTION

Materials. The Korea Herald newspaper was used for paper samples. Parylene C was purchased from Specialty Coating Systems (Indianapolis, IN). Tris(2-carboxyethyl) phosphine (TCEP), 6-mercapto-1-hexanol (MCH), sodium phosphate, phosphate-buffered saline (PBS), potassium ferricyanide, and potassium ferrocyanide were obtained from Sigma-Aldrich. PCR kit was purchased from iNtRON Biotechnology (Seongnam, South Korea). The 50-base oligonucleotides were synthesized by Bioneer Inc. (Daejeon, South Korea) and had a sequence as follows: single-strand probe DNA (ssDNA), 5′-/5ThioMC6-D/TGC CGA ACC TAA AAG TGG TAG TGC ACT GTA TTC AAA GGG AAG TTT TTT GA-3′; target complementary DNA (cDNA), 5′-TC AAA AAA CTT CCC TTT GAA TAC AGT GCA CTA CCA CTT TTA GGT TCG GCA-3′.

Preparation of Paper-Based Electrode. The top and bottom of the paper were totally coated by parylene C. Initially, parylene C (5 g) was placed into a parylene specialty coating system (PDS 2010 Labcoater 2, Speedline Technology, Camdenton, MO) for further vaporization, and pristine paper was placed in a vacuum chamber. The parylene coating process consists of three distinct steps. The first step of vaporization of the solid dimer of parylene C occurred at ∼180 °C, and then, there is cleavage of the dimer at the two methylene−methylene bonds at ∼690 °C to yield the stable monomeric diradical. Finally, as soon as the monomers enter the room temperature of deposition chamber, the monomer of parylene C simultaneously adsorbed and polymerized on the paper. The obtained paper after

DOI: 10.1021/acsami.6b10298
ACS Appl. Mater. Interfaces 2016, 8, 34978−34984

parylene C coating was denoted as the P-paper. A 200-nm-thick gold and silver with 20-nm-thick Ti as an adhesion layer were evaporated through stencil mask using an E-Beam evaporator (KVE T-C500200, South Korea), which forms a three-electrode design on P-paper. We used the gold and silver as working/counter and reference electrodes, respectively.

Immobilization and Hybridization. To prepare the self-assembled capture probe monolayer, 1 μM ssDNA solution involving 10 mM TCEP was deposited directly on the working electrode surface via gold−thiol bonds for 1 h. TCEP was used to break down the disulfide bonds between thiolated DNA. The electrodes were washed with buffer solution several times. MCH monolayer was formed by immersion into MCH aqueous solution (1.4 mM) on working electrode for 1 h to minimize nonspecific binding to the bare gold surface.[38] After immobilization of ssDNA + MCH on the gold electrode, the hybridization reaction was conducted by dropping 50 μL of sodium phosphate buffer solution containing the synthetic cDNA or denatured amplicon of *Escherichia coli* O157:H7 (*E. coli* O157:H7, 384 base pair) at room temperature for 1 h. The electrode was then rinsed thoroughly using the PBS buffer solution. Denaturation of the purified PCR amplicon was performed at 95 °C for 10 min and at 0 °C for 5 min.

Material Characterization. The contact angles (CAs) of pristine newspaper, P-paper, and gold surface were measured using a contact angle meter (Phoenix 300 plus, SEO, South Korea). Scanning electron microscopy (SEM) images were obtained using an S-4800 (Hitachi, Japan) instrument. Prior to SEM measurements, a thin Pt layer (about 5 nm) was deposited on the specimens by magnetron sputtering. Structural properties were analyzed by Raman spectroscopy (NTEGRA spectra, NT-MDT, Russia). The mechanical property changes of both pristine and parylene C coated newspapers were analyzed using universal testing machine (UTM, Instron 5583, Instron Corporation, Canton, MA). An elemental analysis of Ca in the samples was performed by an inductively coupled plasma optical emission spectrometry analysis under standard conditions (iCAP 6300, Thermo Scientific, Waltham, MA). Electrical conductivity was measured by a 4 point probe method (CMT-SR2000, AIT, South Korea).

Electrochemical Measurement. Cyclic voltammetry (CV) and electrochemical impedance spectroscopy (EIS) experiments were performed on PalmSens 3 electrochemical workstation to characterize the step-by-step assembly process and evaluate performance of P-paper electrodes. The electrolyte solution for CV and EIS experiments was 5 mM of $Fe(CN)_6^{3-/4-}$. CV curves were recorded in a range from −0.5 to 0.5 V at a scan rate of 50 mV s^{-1}. EIS measurements were carried out at the equilibrium potential of the redox probe (0.1 V vs Ag) with ac voltage amplitude of 10 mV in the frequency range 0.1 Hz to 10 kHz.

RESULTS AND DISCUSSION

The process used to make P-paper is illustrated schematically in Figure 1a. A continuous and conformal thin film of parylene C was coated onto paper by CVD polymerization of chloro-*p*-xylene. This CVD process consists of three steps: (1) vaporization of the solid dimer at approximately 180 °C, (2) the quantitative pyrolysis of the dimer at about 690 °C to yield stable monomeric diradical chloro-*p*-xylene, and (3) adsorption and polymerization of monomers onto paper to form thin layers of parylene C.[34,39] The parylene C coating formed was uniform, thin, and transparent and, thus, did not obscure print (Figure 1b). SEM was performed to investigate the surface morphologies of pristine newspaper and P-paper (Figure 1c−e). Figure 1c shows the typical morphology of pristine newspaper, in which microfibers are randomly interconnected to generate hierarchical porous structure.[25,40] The conformal coating of parylene C on individual fibers under controlled thickness secured the intrinsic porous feature of paper (Figure 1d,e), compared with the solid wax coating process.[41,42] In order to use P-paper as an electrochemical sensor electrode, we deposited a 200 nm layer of gold and silver on its surface to design a three-electrode pattern using stencil lithography (Figures S1 and S2). To ensure strong attachment of gold and silver on the P-paper surface, 20-nm-thick titanium was used as adhesion layer. P-paper electrodes were designed to be easily torn by hand along perforated lines (Figure S3). We found that P-paper electrodes had excellent flexibility and stability against harsh mechanical stress, such as bending, twisting, or folding; this electrode retains its original state without any cracks or damage (Figure 1f−h). Furthermore, its porous structure was maintained even after metal deposition (Figure S4). A P-paper electrode exhibited a negligible change of electrical conductivity after Scotch tape testing, indicating strong adhesion of the metal layer on P-paper (Table S1).

Examination by Raman spectroscopy revealed a uniform conformal coating of parylene C on the entire cellulose fibers (Figure 2). Representative Raman spectra of thick parylene C

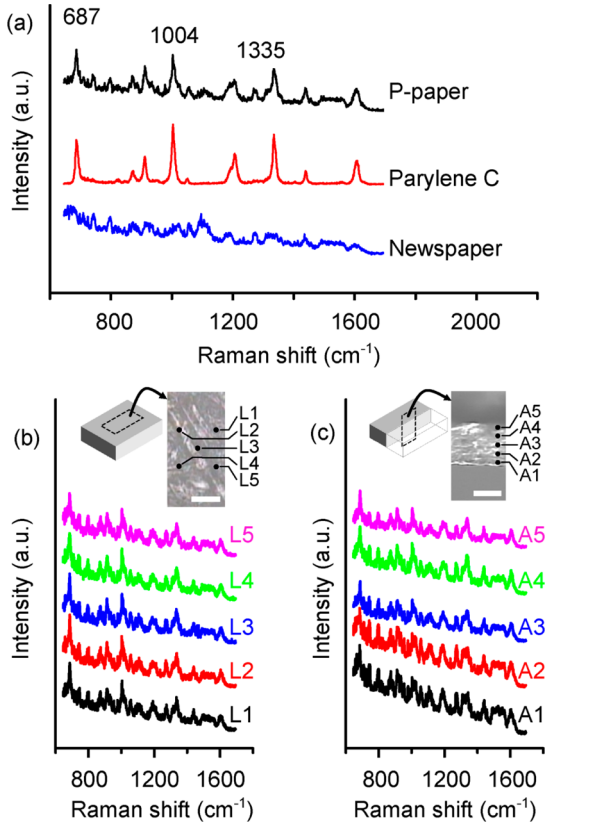

Figure 2. (a) Representative Raman spectra of P-paper, thick parylene C film, and pristine newspaper. (b) Lateral and (c) cross-sectional distribution of Raman spectra on the P-paper. The scale bars for the optical microscope images are 50 μm.

film and pristine paper are shown in Figure 2a. Obviously, the Raman spectrum of the P-paper exhibits characteristic bands of both parylene C and pristine paper. In the Raman spectrum of P-paper, the prominent peaks at ~687, 1004, and 1335 cm^{-1} were attributed to C−Cl stretching vibrations, CH in-plane deformations, and CH_2 wagging/twisting vibrations, respectively, of parylene C.[43−45] Thus, these peaks are used as indicators to confirm the existence of parylene C in cellulose fiber matrices. For examination of the homogeneity of parylene C over cellulose fibers, Raman spectra were obtained at five

DOI: 10.1021/acsami.6b10298
ACS Appl. Mater. Interfaces 2016, 8, 34978−34984

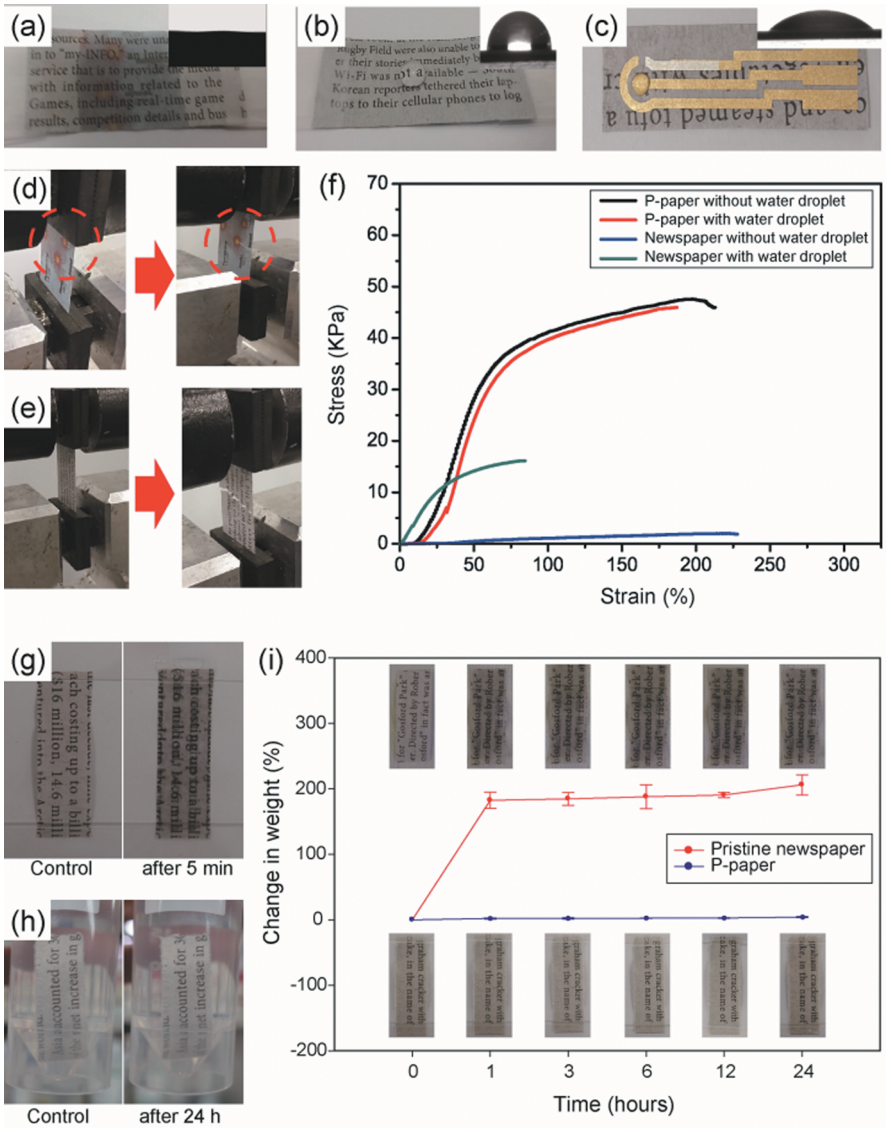

Figure 3. Photographs after dropping a water droplet on (a) pristine newspaper, (b) P-paper, and (c) Au-coated P-paper electrode (Inset is CA images for each from the samples). Photographs of (d) wetted pristine newspaper and (e) wetted P-paper before/after mechanical stretching. (f) Stress–strain curves at vertical pulling of both pristine newspaper and P-paper before/after exposure to water droplets. Water resistance test of (g) pristine newspaper and (h) P-paper using water immersion. (i) Change of weight for pristine newspaper and P-paper as a function of immersion time.

separate points on P-paper (Figure 2b). Moreover, for investigation of diffusion of parylene C inside the porous structure of the cellulose matrix, Raman spectra were also obtained at five points in the cross-sectional area of P-paper (Figure 2c). The characteristic Raman bands of parylene C are clearly discernible in all the Raman spectra, indicating that CVD resulted in the uniform coating of cellulose fibers. Furthermore, all of the colors from the three major peaks were properly attributed to both surface and cross sections of P-paper, indicating uniform coating of cellulose fibers.

Static water CA measurements were performed to investigate the effect of the parylene C coating on paper surface properties (Figure 3a–c). Pristine newspaper was extremely hydrophilic and instantly absorbed water. After parylene C coating, pristine paper became far more hydrophobic; the contact angle increased significantly to approximately 90°. On the other hand, Au coating changed the wettability of P-paper to a CA of 40° (Figure 3c). Consequently, parylene C coating smoothed the surface of the newspaper and provided a nonabsorbing platform that efficiently prevented a drop spreading beyond the confinement of the hydrophilic Au surface. The mechanical properties of pristine paper and P-paper were evaluated in the dry and the wet states (Figure 3d–f and Movie S1). Clearly, the Young's modulus (E) and tensile strength (σ) of dried P-paper were 83.3 and 45.9 kPa, respectively, and were much higher than those of dried pristine paper (E, 45.3 kPa; σ, 16.1 kPa). In contrast, the wetted pristine paper was easily torn. The wettability test was also carried out to investigate the performance of water resilience of P-paper. After immersion of the newspaper into water for 5 min, the significant discoloration of newspaper indicates water absorption because of its porosity and hydrophilicity (Figure 3g). In contrast, P-paper exhibits no color changes and excellent water resiliency even after exposure to water for 24 h due to the conformal coating of parylene C (Figure 3h). The weight changes of both newspaper and P-paper were also observed at different time

DOI: 10.1021/acsami.6b10298
ACS Appl. Mater. Interfaces 2016, 8, 34978–34984

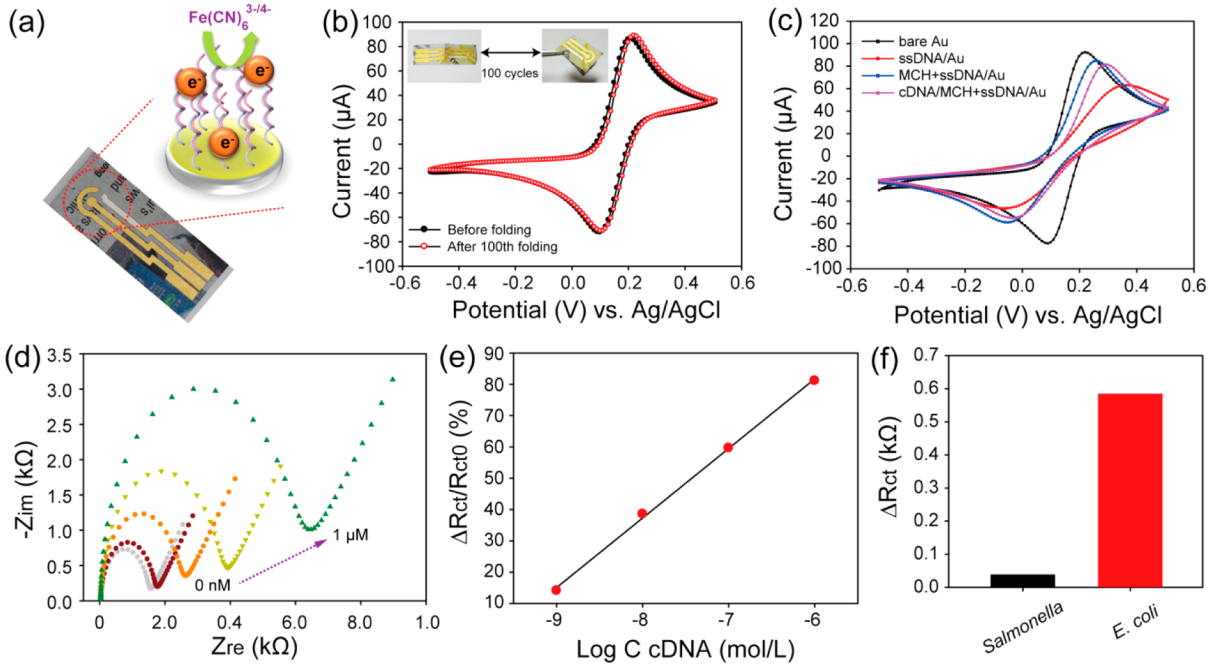

Figure 4. (a) Electrochemical detection of food-borne pathogen using the P-paper electrode. (b) CV curves of P-paper before/after 100 cycles of a fatigue test. (c) CV curves of bare gold electrode, probe ssDNA, ssDNA + MCH- and cDNA/MCH + ssDNA-modified gold electrode (The concentration of cDNA was 10 nM). (d) Nyquist plots of the modified electrode after hybridization with different concentrations of target cDNA. (e) The linear relationship between $\Delta R_{ct}/R_{ct0}$ and logarithmic target concentration. (f) Specificity of P-paper electrodes for detection of *E. coli* O157:H7 against *Salmonella*; the concentration was 5×10^5 CFU mL^{-1}.

frames. After exposure to water, the newspaper rapidly absorbed water and reached saturation only after 1 h while P-paper shows almost no weight changes (Figure 3i). Moreover, the parylene C acted as an efficient barrier layer to block releasing undesirable chemicals from the paper. This is demonstrated via a leaching test of calcium carbonate that used as filler in papers, confirming superiority of parylene coating and elimination of a potential interference in electrochemical sensing (Table S2). These results confirm the merits of parylene C coating, which substantially improves the mechanical properties of paper-based platforms as well as completely blocks penetration of undesirable molecules (e.g., water and calcium carbonate) for flexible and bendable electrochemical device applications (Figure 3g–i and Figure S5).

In order to demonstrate the superior performance of P-paper, we used it as an electrode platform for an electrochemical biosensor used to detect foodborne pathogens (Figure 4a). Foodborne diseases are among the most widespread public health problems, especially in developing countries, because of poor hygiene and limited access to diagnostics and clinical treatment.[46] To address this issue, cost-effective, rapid, and reliable pathogen detection is essentially needed to protect humans from these potential threats. In this regard, our P-paper is suitable for the fabrication of electrochemical pathogen sensors because of its scalable production, disposability, low cost, and environmental friendliness. On P-paper, two gold patterns and one silver pattern were prepared according to the three-electrode system by stencil lithography, in which two gold patterns acted as working and counter electrodes, and a silver pattern acted as a reference electrode (Figure S2).

Prior to fabrication of electrochemical pathogen sensors, the electrochemical behavior of a P-paper electrode was investigated by CV in aqueous 5 mM $Fe(CN)_6^{3-/4-}$ electrolyte solution. The obtained CV curves of a P-paper electrode exhibited a pair of well-defined redox peaks with a peak-to-peak separation (ΔE_p) of 110 mV (Figure 4b), indicating close to reversible electron transfer kinetics.[47] Even after 100 folding cycles, the P-paper electrode produced overlapping CV curves with an electrochemical response of the normal state of P-paper (Figure 4b). As the scan rates increased, the P-paper electrode being folded 100 times exhibited stable and increased CV curves, indicating the flexible electrochemical electrode characteristics of the P-paper (Figure S6).

To examine the sensing performance of an electrochemical biosensor constructed using a P-paper electrode (Figure 4a), we selected *E. coli* O157:H7 as a model foodborne pathogen.[48,49] The ssDNA, which can sensitively recognize its target cDNA of *E. coli* O157:H7, was immobilized on top of a bare Au electrode. The CV technique was used to characterize the electrode at each modification step (Figure 4c). Bare Au electrodes showed a couple of reversible redox peaks with ΔE_p of 100 mV. After immobilization of the probe ssDNA and blocking with the MCH monolayer, peak current decreased significantly, and ΔE_p (310 mV) increased versus the bare Au electrode due to the repulsion between $Fe(CN)_6^{3-/4-}$ by negatively charged ssDNA. Target cDNA was subsequently hybridized with probe ssDNA on the electrode, which led to a continual decrease in peak current and increase in ΔE_p to 330 mV. These results indicate that probe ssDNA was successfully immobilized on the surface of electrode and hybridized with target cDNA. In order to better investigate the sensing performance of P-paper electrodes, electrochemical impedance spectroscopy (EIS) was also performed using $Fe(CN)_6^{3-/4-}$ as indicator. The sensitivity of the paper-based electrode for *E. coli* was evaluated by measuring the EIS parameter and fitting with a Randle equivalent circuit model (Figure S7), where R_s represents internal resistance of the circuit, R_{ct} and C_{dl} are

DOI: 10.1021/acsami.6b10298
ACS Appl. Mater. Interfaces 2016, 8, 34978–34984

charge transfer resistance and double layer capacitance at the electrode, respectively, and Z_W is associated with Warburg impedance which is related to diffusion processes of the redox probe.[50] Nyquist plots in Figure 4d show the gradual increase in R_{ct} that occurred on increasing target cDNA concentration. This indicates target cDNA bound to probe ssDNA immobilized on the electrode to produce a more negatively charged surface that attenuates the electron transfer kinetics of $Fe(CN)_6^{3-/4-}$. Normalized R_{ct} changes (namely $\Delta R_{ct}/R_{ct0}$) between the ssDNA/MCH (R_{ct0}) and after cDNA hybridization (R_{ct}) were used as measurement signals. As shown in Figure 4e, a good linear relationship (R^2 = 0.9988) was observed between R_{ct} and the logarithm of target cDNA concentration with a detection limit of 0.16 nM (defined as S/N = 3), which was comparable to other reported electrochemical detection methods for pathogenic DNA (Table S3). In addition, the specificity of P-paper-based electrodes was also evaluated (Figure 4f). After hybridization with a PCR sample containing *Salmonella* DNA sequence, the change of R_{ct} value was negligible, indicating little hybridization. This P-paper could be readily disposed by simply burning it after cDNA detection (Movie S2) and, thus, provides a reliable, low-cost, and disposable means of measuring the concentrations of target biomolecules.

CONCLUSIONS

We demonstrated a straightforward and scalable process for fabrication of newspaper-based sensing platforms by CVD of parylene C and a subsequent electrode patterning process. The resulting P-paper electrodes exhibited strong water resistance and a high mechanical integrity. A parylene C deposition enabled a uniform conformal coating and porous structure. P-paper electrodes showed superior electrochemical performances for the application of biosensors. We also examined the biosensing performance for detection of pathogenic *E. coli* O157:H7 based on DNA hybridization detection. The P-paper electrode showed high sensitivity and specific detection of pathogenic *E. coli* O157:H7. The P-paper electrodes developed in this work could provide reliable, low-cost, and disposable sensing platforms for point-of-care testing biosensor systems.

ASSOCIATED CONTENT

Supporting Information

The Supporting Information is available free of charge on the ACS Publications website at DOI: 10.1021/acsami.6b10298.

Additional details regarding fabrication and design, photographs and SEM images of the electrodes, and additional figures detailing physical properties and sensor performance (PDF)

Movie showing the wettability properties of P-paper (AVI)

Movie showing P-paper buurning after cDNA detection for disposal (AVI)

AUTHOR INFORMATION

Corresponding Authors

*E-mail: sjlee@nnfc.re.kr.

*E-mail: bgchoi@kangwon.ac.kr.

*E-mail: kglee@nnfc.re.kr.

ORCID

Minjeong Jang: 0000-0002-4047-4716

Kyoung G. Lee: 0000-0003-2691-0910

Author Contributions

†M.Y. and S.W.J. contributed equally to this work.

Notes

The authors declare no competing financial interest.

ACKNOWLEDGMENTS

This work was supported by BioNano Health-Guard Research Center funded by the Ministry of Science, ICT & Future Planning (MSIP) of Korea as Global Frontier Project (Grant Number H-GUARD_2013M3A6B2078945 and 2014M3A6B2060489). This research was also supported by the Public Welfare & Safety research program through the National Research Foundation of Korea (NRF) funded by the Ministry of Science, ICT and Future Planning (MSIP) of Korea (NRF-2013M3A2A1073991 and No. 2014R1A5A2010008) and a grant (The core project-02) from Gumi Core Components and Materials Technology Development Program of the Gumi Regional Government, 2016.

REFERENCES

(1) Fiori, G.; Bonaccorso, F.; Iannaccone, G.; Palacios, T.; Neumaier, D.; Seabaugh, A.; Banerjee, S. K.; Colombo, L. Electronics Based on Two-Dimensional Materials. *Nat. Nanotechnol.* **2014**, *9*, 768−779.

(2) Rus, D.; Tolley, M. T. Design, Fabrication and Control of Soft Robots. *Nature* **2015**, *521*, 467−475.

(3) Inui, T.; Koga, H.; Nogi, M.; Komoda, N.; Suganuma, K. A Miniaturized Flexible Antenna Printed on a High Dielectric Constant Nanopaper Composite. *Adv. Mater.* **2015**, *27*, 1112−1116.

(4) Gao, W.; Emaminejad, S.; Nyein, H. Y. Y.; Challa, S.; Chen, K.; Peck, A.; Fahad, H. M.; Ota, H.; Shiraki, H.; Kiriya, D.; Lien, D.-H.; Brooks, G. A.; Davis, R. W.; Javey, A. Fully Integrated Wearable Sensor Arrays for Multiplexed *In Situ* Perspiration Analysis. *Nature* **2016**, *529*, 509−514.

(5) Heikenfeld, J. Bioanalytical devices: Technological Leap for Sweat Sensing. *Nature* **2016**, *529*, 475−476.

(6) Windmiller, J. R.; Wang, J. Wearable Electrochemical Sensors and Biosensors: A Review. *Electroanalysis* **2013**, *25*, 29−46.

(7) Kahn, N.; Lavie, O.; Paz, M.; Segev, Y.; Haick, H. Dynamic Nanoparticle-Based Flexible Sensors: Diagnosis of Ovarian Carcinoma from Exhaled Breath. *Nano Lett.* **2015**, *15*, 7023−7028.

(8) Segev-Bar, M.; Haick, H. Flexible Sensors Based on Nanoparticles. *ACS Nano* **2013**, *7*, 8366−8378.

(9) Kim, B.; Lu, Y.; Kim, T.; Han, J.-W.; Meyyappan, M.; Li, J. Carbon Nanotube Coated Paper Sensor for Damage Diagnosis. *ACS Nano* **2014**, *8*, 12092−12097.

(10) Han, J.-W.; Kim, B.; Li, J.; Meyyappan, M. Carbon Nanotube Based Humidity Sensor on Cellulose Paper. *J. Phys. Chem. C* **2012**, *116*, 22094−22097.

(11) Kim, Y.; Jang, G.; Lee, T. S. New Fluorescent Metal-Ion Detection Using a Paper-Based Sensor Strip Containing Tethered Rhodamine Carbon Nanodots. *ACS Appl. Mater. Interfaces* **2015**, *7*, 15649−15657.

(12) Gimenez, A. J.; Yáñez-Limón, J. M.; Seminario, J. M. Paper-Based Photoconductive Infrared Sensor. *J. Phys. Chem. C* **2011**, *115*, 18829−18834.

(13) Mahadeva, S. K.; Walus, K.; Stoeber, B. Paper as a Platform for Sensing Applications and Other Devices: A Review. *ACS Appl. Mater. Interfaces* **2015**, *7*, 8345−8362.

(14) Mazzeo, A. D.; Kalb, W. B.; Chan, L.; Killian, M. G.; Bloch, J.-F.; Mazzeo, B. A.; Whitesides, G. M. Paper-Based, Capacitive Touch Pads. *Adv. Mater.* **2012**, *24*, 2850−2856.

(15) Hammock, M. L.; Chortos, A.; Tee, B. C.-K.; Tok, J. B.-H.; Bao, Z. The Evolution of Electronic Skin (E-Skin): A Brief History, Design Considerations, and Recent Progress. *Adv. Mater.* **2013**, *25*, 5997−6038.

DOI: 10.1021/acsami.6b10298
ACS Appl. Mater. Interfaces 2016, 8, 34978−34984

(16) Russo, A.; Ahn, B. Y.; Adams, J. J.; Duoss, E. B.; Bernhard, J. T.; Lewis, J. A. Pen-on-Paper Flexible Electronics. *Adv. Mater.* **2011**, *23*, 3426−3430.
(17) Esquivel, J. P.; Del Campo, F. J.; Gómez de la Fuente, J. L.; Rojas, S.; Sabaté, N. Microfluidic Fuel Cells on PaperMeeting the Power Needs of Next Generation Lateral Flow Devices. *Energy Environ. Sci.* **2014**, *7*, 1744−1749.
(18) Zheng, G.; Hu, L.; Wu, H.; Xie, X.; Cui, Y. Paper Supercapacitors by a Solvent-Free Drawing Method. *Energy Environ. Sci.* **2011**, *4*, 3368−3373.
(19) Mirica, K. A.; Weis, J. G.; Schnorr, J. M.; Esser, B.; Swager, T. M. Mechanical Drawing of Gas Sensors on Paper. *Angew. Chem., Int. Ed.* **2012**, *51*, 10740−10745.
(20) Parolo, C.; Merkoçi, A. Paper-Based Nanobiosensors for Diagnostics. *Chem. Soc. Rev.* **2013**, *42*, 450−457.
(21) Dungchai, W.; Chailapakul, O.; Henry, C. S. Electrochemical Detection for Paper-Based Microfluidics. *Anal. Chem.* **2009**, *81*, 5821−5826.
(22) Gullapalli, H.; Vemuru, V. S. M.; Kumar, A.; Botello-Mendez, A.; Vajtai, R.; Terrones, M.; Nagarajaiah, S.; Ajayan, P. M. Flexible Piezoelectric ZnO−Paper Nanocomposite Strain Sensor. *Small* **2010**, *6*, 1641−1646.
(23) Liana, D. D.; Raguse, B.; Wieczorek, L.; Baxter, G. R.; Chuah, K.; Gooding, J. J.; Chow, E. Sintered Gold Nanoparticles as an Electrode Material for Paper-Based Electrochemical Sensors. *RSC Adv.* **2013**, *3*, 8683−8691.
(24) Topgaard, D.; Söderman, O. Diffusion of Water Absorbed in Cellulose Fibers Studied with ^{1}H-NMR. *Langmuir* **2001**, *17*, 2694−2702.
(25) Tobjörk, D.; Österbacka, R. Paper Electronics. *Adv. Mater.* **2011**, *23*, 1935−1961.
(26) Chitnis, G.; Ziaie, B. Waterproof Active Paper via Laser Surface Micropatterning of Magnetic Nanoparticles. *ACS Appl. Mater. Interfaces* **2012**, *4*, 4435−4439.
(27) Jung, Y. H.; Chang, T.-H.; Zhang, H.; Yao, C.; Zheng, Q.; Yang, V. W.; Mi, H.; Kim, M.; Cho, S. J.; Park, D.-W.; Jiang, H.; Lee, J.; Qiu, Y.; Zhou, W.; Cai, Z.; Gong, S.; Ma, Z. High-Performance Green Flexible Electronics Based on Biodegradable Cellulose Nanofibril Paper. *Nat. Commun.* **2015**, *6*, 7170.
(28) Zheng, Y.; He, Z.; Gao, Y.; Liu, J. Direct Desktop Printed-Circuits-on-Paper Flexible Electronics. *Sci. Rep.* **2013**, *3*, 1786.
(29) Jin, C.; Jiang, Y.; Niu, T.; Huang, J. Cellulose-Based Material with Amphiphobicity to Inhibit Bacterial Adhesion by Surface Modification. *J. Mater. Chem.* **2012**, *22*, 12562−12567.
(30) Yetisen, A. K.; Safwan Akram, M.; Lowe, C. R. Paper-Based Microfluidic Point-of-Care Diagnostic Devices. *Lab Chip* **2013**, *13*, 2210−2251.
(31) Lessing, J.; Glavan, A. C.; Walker, S. B.; Keplinger, C.; Lewis, J. A.; Whitesides, G. M. Inkjet Printing of Conductive Inks with High Lateral Resolution on Omniphobic "R(F) Paper" for Paper-Based Electronics and MEMS. *Adv. Mater.* **2014**, *26*, 4677−4682.
(32) Samyn, P. Wetting and Hydrophobic Modification of Cellulose Surfaces for Paper Applications. *J. Mater. Sci.* **2013**, *48*, 6455−6498.
(33) Cate, D. M.; Adkins, J. A.; Mettakoonpitak, J.; Henry, C. S. Recent Developments in Paper-Based Microfluidic Devices. *Anal. Chem.* **2015**, *87*, 19−41.
(34) Tan, C. P.; Craighead, H. G. Surface Engineering and Patterning Using Parylene for Biological Applications. *Materials* **2010**, *3*, 1803−1832.
(35) You, J. B.; Yoo, Y.; Oh, M. S.; Im, S. G. Simple and Reliable Method to Incorporate the Janus Property onto Arbitrary Porous Substrates. *ACS Appl. Mater. Interfaces* **2014**, *6*, 4005−4010.
(36) Baxamusa, S. H.; Im, S. G.; Gleason, K. K. Initiated and Oxidative Chemical Vapor Deposition: A Scalable Method for Conformal and Functional Polymer Films on Real Substrates. *Phys. Chem. Chem. Phys.* **2009**, *11*, 5227−5240.
(37) Sreenivasan, R.; Gleason, K. K. Overview of Strategies for the CVD of Organic Films and Functional Polymer Layers. *Chem. Vap. Deposition* **2009**, *15*, 77−90.
(38) Wong, E. L. S.; Chow, E.; Gooding, J. J. DNA Recognition Interfaces: The Influence of Interfacial Design on the Efficiency and Kinetics of Hybridization. *Langmuir* **2005**, *21*, 6957−6965.
(39) Fortin, J. B.; Lu, T.-M. Chemical Vapor Deposition Polymerization. *The Growth and Properties of Parylene Thin Films*; Kluwer Academic Publishers, Norwell, MA, 2004; pp 41−55.
(40) Moon, R. J.; Martini, A.; Nairn, J.; Simonsen, J.; Youngblood, J. Cellulose Nanomaterials Review: Structure, Properties and Nanocomposites. *Chem. Soc. Rev.* **2011**, *40*, 3941−3994.
(41) de Araujo, W. R.; Paixão, T. R. L. C. Fabrication of Disposable Electrochemical Devices Using Silver Ink and Office Paper. *Analyst* **2014**, *139*, 2742−2747.
(42) Marques, A. C.; Santos, L.; Costa, M. N.; Dantas, J. M.; Duarte, P.; Gonçalves, A.; Martins, R.; Salgueiro, C. A.; Fortunato, E. Office Paper Platform for Bioelectrochromic Detection of Electrochemically Active Bacteria using Tungsten Trioxide Nanoprobes. *Sci. Rep.* **2015**, *5*, 9910.
(43) Mathur, M. S.; Weir, N. A. Laser Raman and Infrared Spectrum of Poly-*p*-Xylylene. *J. Mol. Struct.* **1973**, *15*, 459−463.
(44) Agarwal, U. P.; Ralph, S. A. FT-Raman Spectroscopy of Wood: Identifying Contributions of Lignin and Carbohydrate Polymers in the Spectrum of Black Spruce (Picea Mariana). *Appl. Spectrosc.* **1997**, *51*, 1648−1655.
(45) Colthup, N. B.; Daly, L. H.; Wiberley, S. E. *Introduction to Infrared and Raman Spectroscopy*; Academic Press: San Diego, CA, 1990.
(46) Grace, D. Food Safety in Low and Middle Income Countries. *Int. J. Environ. Res. Public Health* **2015**, *12*, 10490−10507.
(47) Bard, A. J.; Faulkner, L. R. Electrochemical Methods. *Fundamentals and Applications*; Wiley: New York, 2001.
(48) Eppinger, M.; Mammel, M. K.; Leclerc, J. E.; Ravel, J.; Cebula, T. A. Genomic Anatomy of *Escherichia coli* O157:H7 Outbreaks. *Proc. Natl. Acad. Sci. U. S. A.* **2011**, *108*, 20142−201427.
(49) Rangel, J. M.; Sparling, P. H.; Crowe, C.; Griffin, P. M.; Swerdlow, D. L. Epidemiology of *Escherichia coli* O157:H7 Outbreaks, United States, 1982−2002. *Emerging Infect. Dis.* **2005**, *11*, 603−609.
(50) Randviir, E. P.; Banks, C. E. Electrochemical Impedance Spectroscopy: An Overview of Bioanalytical Applications. *Anal. Methods* **2013**, *5*, 1098−1115.

DOI: 10.1021/acsami.6b10298
ACS Appl. Mater. Interfaces 2016, 8, 34978−34984